ORGANOMETALLICS

pubs.acs.org/Organometallics Article

Probing for Four-Coordinate Zerovalent Iron in a π-Acidic Ligand Field: A Functional Source of FeL_4 Enabled by Labile Dinitrogen Binding

Myles J. Drance, Shuai Wang, Milan Gembicky, Arnold L. Rheingold, and Joshua S. Figueroa*

Cite This: *Organometallics* 2020, 39, 3394−3402 Read Online

ACCESS | Metrics & More | Article Recommendations | Supporting Information

ABSTRACT: It has long been recognized that the first intermediate in chemical reactions mediated by $Fe(CO)_5$ is $Fe(CO)_4$. However, the extreme instability of this unsaturated, high-spin species has hampered detailed structural and stoichiometric reactivity studies. The previously reported heteroleptic complex $Fe(N_2)(CO)_2(CNAr^{Tripp2})_2$ (Ar^{Tripp2} = 2,6-(2,4,6-(*i*-Pr)$_3C_6H_2)_2C_6H_3$), which is isolobal to $Fe(CO)_5$, is shown here to possess a labile dinitrogen ligand that allows it to perform reactions analogous to $Fe(CO)_4$. Specifically, $Fe(N_2)(CO)_2(CNAr^{Tripp2})_2$ oxidatively adds dihydrogen, white phosphorus, and the Si−H bonds of triethylsilane and phenylsilane readily at room temperature and also binds tetrahydrofuran in the absence of N_2. Accordingly, $Fe(N_2)(CO)_2(CNAr^{Tripp2})_2$ effectively serves as a masked form of $Fe(CO)_4$, allowing for well-defined reactivity and structurally characterizable reaction products.

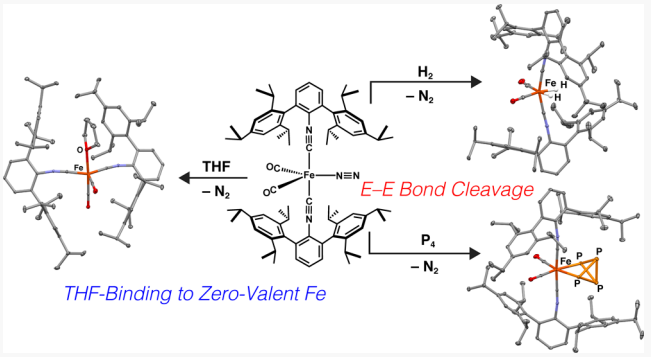

INTRODUCTION

The binary mononuclear iron carbonyl, $Fe(CO)_4$, has long been studied as a transient species and reaction intermediate in organometallic chemistry.[1−3] While $Fe(CO)_4$ was first mentioned in the literature in 1891 as the product formed upon passage of carbon monoxide over activated iron,[4] more accurate measurements in a subsequent report corrected the formula of this volatile iron carbonyl to $Fe(CO)_5$.[5] The existence of $Fe(CO)_4$ was postulated again in 1905 as the intermediate after CO dissociation in the decomposition of $Fe(CO)_5$ to $Fe_2(CO)_9$ in sunlight, the first reported photoreaction involving a metal carbonyl.[5,6] Following this observation, the photochemistry of $Fe(CO)_5$ was thoroughly explored throughout the 20th century, leading to the utilization of photogenerated $Fe(CO)_4$ as a reactive protagonist in numerous catalytic processes such as olefin hydroformylation, hydrogenation, hydrosilylation, and isomerization.[7−11]

While unstable under ambient conditions, $Fe(CO)_4$ has nonetheless been widely investigated by an array of techniques including cryogenic matrix isolation,[12,13] time-resolved infrared spectroscopy (TRIR),[14,15] and electron diffraction,[16,17] which has allowed for a considerable understanding of its geometric and electronic structure properties.[1−3,18−20] Given that a d^8 electronic configuration possesses first-order Jahn−Teller instability in an idealized tetrahedral ligand field, Burdett and Hoffmann predicted that $Fe(CO)_4$ would adopt a C_{2v}, so-called "saw-horse", ground-state geometry (Scheme 1). Consequently, the two highest-lying metal-based orbitals are close in energy leading to a high-spin S = 1 electronic configuration, unusual for a metal center bound exclusively by strong-field ligands.[21−23] Poliakoff provided the first experimental evidence of C_{2v}-symmetric $Fe(CO)_4$ in various matrices at 20 K by correlating bond angles derived from IR spectroscopy with geometrical features predicted using theoretical methods.[13] Notably, the combined experimental and theoretical treatment of $Fe(CO)_4$ has concluded that it possesses a triplet $^3B_2$ ground state with an energetically accessible singlet $^1A_1$ excited state.[18] This finding has rendered

Scheme 1. Traditional Photolytic Pathway to Iron Tetracarbonyl

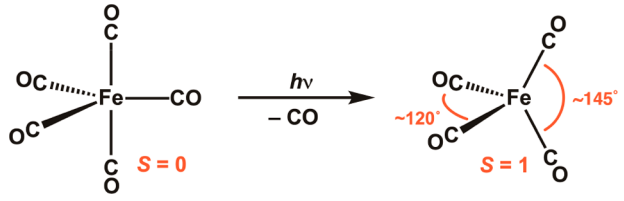

Received: July 20, 2020
Published: September 10, 2020

Downloaded via UNIV OF CALIFORNIA SAN DIEGO on October 28, 2020 at 17:52:57 (UTC).
See https://pubs.acs.org/sharingguidelines for options on how to legitimately share published articles.

ACS Publications © 2020 American Chemical Society

https://dx.doi.org/10.1021/acs.organomet.0c00487
Organometallics 2020, 39, 3394−3402

this simple species an important case study for examining the effect of spin-state changes on structure and reactivity.[20,24−28]

The extensive study of $Fe(CO)_4$ in various cryogenic matrices has revealed dramatic reaction chemistry, which includes methane (CH_4) and xenon (Xe) binding.[27,28] However, the short lifetime and highly reactive nature of this species and its reaction products have precluded the acquisition of detailed spectroscopic and structural data.[12,19,28] A notable exception to this has been the unequivocal structure determination of the excited $^1A_1$ electronic state of $Fe(CO)_4$ in the gas phase using ultrafast electron diffraction.[17] To better understand the electronic structure and reactivity of $Fe(CO)_4$ in the solution phase, a number of four-coordinate, formally iron(0) complexes have been prepared utilizing olefins, *N*-heterocyclic carbenes (NHCs), and/or phosphines as ancillary ligands (Chart 1).

Chart 1. (Top) Selected Examples of Structurally-Characterized Four-Coordinate Zerovalent Iron Complexes; (Bottom) Dinitrogen-Stabilized *m*-Terphenyl Isocyanide Complexes of Zerovalent Iron

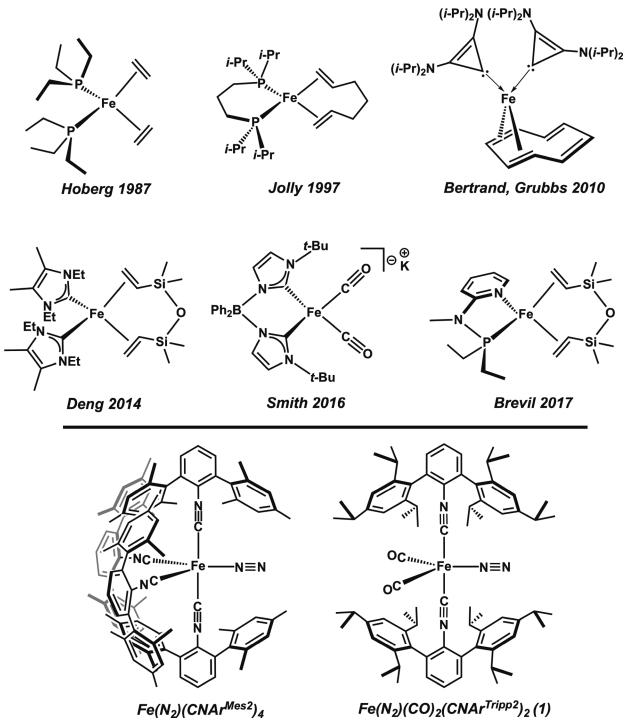

However, as these ligands are far stronger σ-donors than CO, or provide only one π-backbonding interaction, these differences have resulted in d-orbital splitting and electronic configurations that are dissimilar to that of $Fe(CO)_4$. Consequently, the reaction chemistry of such complexes is often divergent from that associated with this simple tetracarbonyl species.[29−35]

Over the past several years, our group has focused on generating kinetically stabilized analogues of some of the classical unsaturated binary metal carbonyls through the use of sterically encumbering *m*-terphenyl isocyanides.[36−39] Isocyanides are well recognized as isolobal surrogates to CO as they provide a σ-donor functionality along with two orthogonal π-backbonding interactions. While organoisocyanides are both stronger σ-donors and weaker π-acids relative to CO,[40,41] they generate a more precisely matched electronic structure environment for binary metal carbonyl mimics than other ancillary ligands. Accordingly, we have shown that *m*-terphenyl isocyanide mimics of $Mn(CO)_5$,[39,42] $Co(CO)_4$,[38,43] and $Ni(CO)_3$[37,44] display the structural, spectroscopic, and reactivity characteristics of their homoleptic carbonyl counterparts. For the case of an isocyanide mimic of $Fe(CO)_4$, we have previously reported the isolation of the tetraisocyanide complex, $Fe(N_2)(CNAr^{Mes2})_4$ (Ar^{Mes2} = 2,6-(2,4,6-$Me_3C_6H_2)_2C_6H_3$), which is ostensibly formed by N_2 trapping of the unobserved species $[Fe(CNAr^{Mes2})_4]$ in solution (Chart 1). This N_2-trapping process is similar to that employed by Whitmire for the solution phase trapping of $Fe(CO)_4$ by organophosphine ligands.[45] While $Fe(N_2)(CNAr^{Mes2})_4$ provided us with a potential access point to the chemistry of an FeL_4 species supported by isocyanide ligands, this complex did not display good thermal stability properties under ambient conditions. Indeed, although isolable at low temperature, $Fe(N_2)(CNAr^{Mes2})_4$ was observed to fully decompose over the course of 4 h at room temperature in solution via an intramolecular ligand C−H activation pathway.[46] This degree of C−H bond activation reactivity mimicked that of $Fe(CO)_4$, but did not allow for a conveniently handled system to further explore reactivity pathways.

More recently, we reported the iron-dinitrogen complex, $Fe(N_2)(CO)_2(CNAr^{Tripp2})_2$ (**1**; Ar^{Tripp2} = 2,6-(2,4,6-(*i*-$Pr)_3C_6H_2)_2C_6H_3$),[47] featuring a mixed carbonyl and isocyanide ligand set (Chart 1). Relative to $Fe(N_2)(CNAr^{Mes2})_4$, $Fe(N_2)(CO)_2(CNAr^{Tripp2})_2$ (**1**) displays enhanced thermal stability in solution at room temperature. This increased stability, which is enabled by the combination of increased steric protection of the Ar^{Tripp2} ligands and electronic stabilization provided by the two CO ligands, has allowed the reaction chemistry of $Fe(N_2)(CO)_2(CNAr^{Tripp2})_2$ to be readily assessed. Accordingly, in this report, we present a more detailed description of $Fe(N_2)(CO)_2(CNAr^{Tripp2})_2$ (**1**) and the ability of the N_2 ligand to be readily displaced by other substrates. We demonstrate that this N_2-stabilized FeL_4 complex can successfully display small-molecule binding and activation chemistry in analogy to that of $Fe(CO)_4$.

RESULTS AND DISCUSSION

The terminal dinitrogen complex $Fe(N_2)(CO)_2(CNAr^{Tripp2})_2$ (**1**) can be generated in good yield by oxidation of the formally Fe(-II) precursor $K_2[Fe(CO)_2(CNAr^{Tripp2})_2]$ with molecular iodine (I_2) in Et_2O solution under an N_2 atmosphere (Scheme 2).[47] As in the case of $Fe(N_2)(CNAr^{Mes2})_4$, it is likely that the four-coordinate iron(0) species, $Fe(CO)_2(CNAr^{Tripp2})_2$, is formed fleetingly and is rapidly intercepted by N_2. Notably, when the oxidation of $K_2[Fe(CO)_2(CNAr^{Tripp2})_2]$ is performed under similar conditions in the absence of N_2, an intractable mixture is obtained from which only free $CNAr^{Tripp2}$ and the tricarbonyl complex, $Fe(CO)_3(CNAr^{Tripp2})_2$,[47] are identifiable by ^1H NMR and FTIR spectroscopy. Accordingly, despite the more encumbering nature of the $CNAr^{Tripp2}$ ligands and the increased π-acidity properties of the CO ligands, an electronic environment in which a four-coordinate zerovalent FeL_4 complex can be stabilized toward isolation is not achieved. In this respect, it is important to note that, to date, isolable zerovalent FeL_4 complexes all possess strongly σ-donating ancillary ligands. This fact suggests that increasing ligand-field strengths via strong σ-donation, rather than by the presence of significant π-backbonding interactions, may be critical for stabilizing a four-

https://dx.doi.org/10.1021/acs.organomet.0c00487
Organometallics 2020, 39, 3394−3402

Scheme 2. Synthesis and Decomposition of the Dinitrogen Complex 1

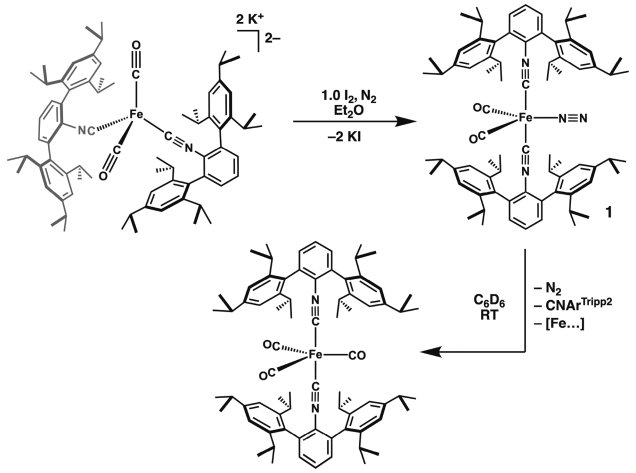

coordinate d^8 iron center. This notion also further highlights the inherent instability of $Fe(CO)_4$, for which electronic, rather than steric, features of the system clearly serve as the origin of its short lifetime and inaccessibility toward isolation.

Orange-yellow crystals of $Fe(N_2)(CO)_2(CNAr^{Tripp2})_2$ (**1**) can be readily obtained upon crystallization from 20:1 *n*-pentane/benzene mixture at −35 °C. X-ray structural determination of **1** revealed that it adopts a trigonal bipyramidal coordination geometry in the solid state, with axial isocyanides and an equatorial plane consisting of the two CO ligands and N_2 (Figure 1). The internuclear distance

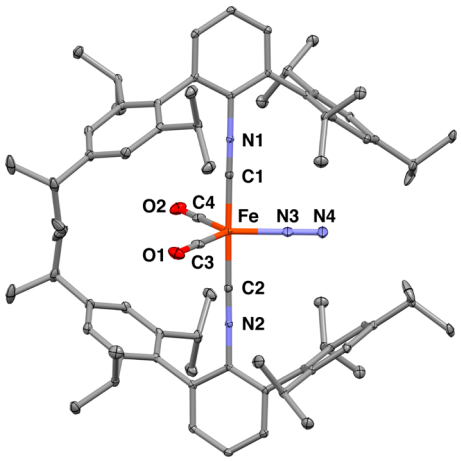

Figure 1. Molecular structure of $Fe(N_2)(CO)_2(CNAr^{Tripp2})_2$.[47] Selected bond distances (Å): Fe−N3 = 1.8850(33), N3−N4 = 1.1059(41).

between the Fe center and the bound nitrogen atom (d(Fe−N_α = 1.8850(33) Å) is long relative to other iron terminal dinitrogen complexes listed in the Cambridge Structural Database ($d(Fe-N_\alpha)_{av}$ = 1.821(±0.037) Å),[48] thereby suggesting inefficient d(Fe) → $\pi^*(N_2)$ backbonding interactions. This notion is supported by a short N−N distance of 1.1059(41) Å in the solid-state structure of **1**, further indicating limited activation of the bound N_2 ligand. Such a low degree of N_2 activation in complex **1** is unsurprising, given that the strongly π-acid character of both the CO and isocyanide coligands serve to remove electron density from the Fe center. In fact, the ν_{NN} stretch of the N_2 ligand of **1** occurs at 2194 cm^{-1}, which is considerably higher in energy than those reported previously for structurally characterized iron terminal dinitrogen complexes (ν_{NN} = 2008−2143 cm^{-1}).[49] As a point of comparison the ν_{NN} of **1** is found at nearly 130 cm^{-1} higher frequency than the more electron rich tetraisocyanide complex $Fe(N_2)(CNAr^{Mes2})_4$[46] and ca. 50 cm^{-1} lower than $Fe(N_2)(CO)_4$, which has only been observed under cryogenic matrix conditions.[13] This spectroscopic ordering is consistent with the intermediate σ-donor/π-acceptor ratio of a mixed CO/isocyanide ligand set,[40] and it suggests that the electron density at iron in **1** more closely resembles that of $Fe(N_2)(CO)_4$ than the tetraisocyanide complex $Fe(N_2)(CNAr^{Mes2})_4$. Importantly, all three of these isolobal species adopt analogous trigonal bipyramidal coordination geometries, with N_2 bound at an equatorial site. It is important to note that $Fe(N_2)(CO)_4$ was originally proposed to feature an axially bound N_2 ligand, but this structural assignment was later revised to one where equatorial coordination of N_2 is preferred.[13,50] In terms of its bulk purity, repeated microanalysis attempts on crystalline samples of **1** unfortunately indicate the likely presence of substoichiometric inclusion of KI. However, this impurity does not affect the chemistry accessible to complex **1**, especially as they pertain to the known reactivity patterns of $Fe(CO)_4$.

In contrast to the tetraisocyanide dinitrogen complex, $Fe(N_2)(CNAr^{Mes2})_4$, complex **1** shows reasonable stability in benzene, *n*-pentane and Et_2O solution under an N_2 atmosphere and can be handled in these solvents at room temperature without noticeable diminution in spectroscopic purity over the course of approximately 30 min. However, allowing **1** to stir in C_6D_6 solution at room temperature for 24 h results in its gradual decay to free $CNAr^{Tripp2}$ and the tricarbonyl complex, $Fe(CO)_3(CNAr^{Tripp2})_2$,[47] which likely forms via an intermolecular ligand redistribution process upon dissociation of N_2 (Scheme 2). Conversely, $Fe(N_2)(CNAr^{Mes2})_4$ decomposes through an intramolecular ligand degradation pathway within ca. 4 h, and $Fe(N_2)(CO)_4$ has a lifetime of significantly less than one second at room temperature.[46,50] Evidently, the electron withdrawing properties of CO along with the larger steric profile of $CNAr^{Tripp2}$ discourage intramolecular decomposition processes for **1**, while also kinetically stabilizing the coordination of N_2 to a greater extent than either $Fe(N_2)(CNAr^{Mes2})_4$ or $Fe(N_2)(CO)_4$.

Whereas complex **1** persists in relatively nonpolar solvents under an N_2 atmosphere, when placed in THF solution and subjected to a vacuum, a distinctive darkening of the medium to a brown color is observed. This color change indicated the formation of a new species, as it contrasts with that observed for the decomposition of **1** to the tricarbonyl complex $Fe(CO)_3(CNAr^{Tripp2})_2$, which is bright yellow and results in a lightening of the reaction mixture. To isolate this darker-colored compound, complex **1** was placed under an argon atmosphere and stored overnight at −35 °C in a *n*-pentane/THF mixture. This procedure deposited yellow-brown single crystals, which were determined by X-ray diffraction to be the THF-adduct $Fe(THF)(CO)_2(CNAr^{Tripp2})_2$ (**2**) arising from the loss of N_2 (Scheme 3). As shown in Figure 2, complex **2** undergoes a substantial rearrangement of the ancillary ligand set relative to **1**, such that the equatorial plane now consists of two isocyanides and one CO ligand, while axial positions are occupied by THF and the other carbonyl ligand. For a five-

https://dx.doi.org/10.1021/acs.organomet.0c00487
Organometallics 2020, 39, 3394−3402

Scheme 3. Reversible Formation of Complex 2 via Substitution of N_2 by THF

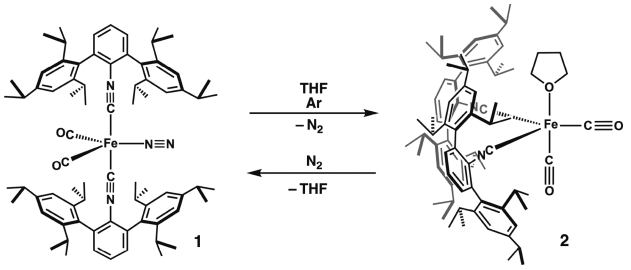

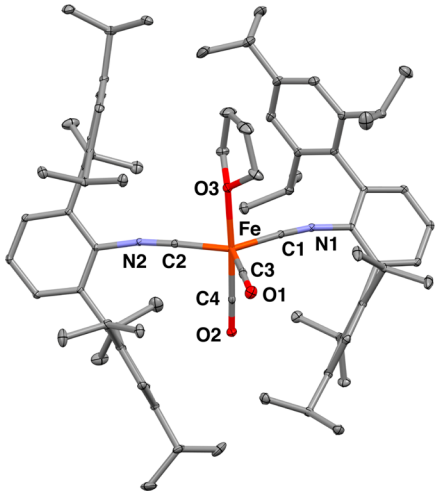

Figure 2. Molecular structure of $Fe(THF)(CO)_2(CNAr^{Tripp2})_2$ (**2**).

coordinate, nominally trigonal bipyramidal complex, this rearrangement likely occurs to maximize π-backbonding interactions from the filled iron $d_{x^2-y^2}$ and d_{xy}, orbitals by placing three π-acidic ligands within the equatorial plane. Most notably, while there are 291 crystallographically characterized iron complexes featuring a THF ligand in the Cambridge Structural Data Base,[48] to our knowledge, complex **2** is the only example where THF binds to a formally zerovalent Fe center. We interpret this unusual observation as further reflection of the instability of the $[Fe(CO)_2(CNR)_2]$ fragment and the seeming inability of the encumbering $CNAr^{Tripp2}$ ligands to provide a stabilizing secondary bonding contact to the zerovalent Fe center via π-arene interactions. As we have shown previously, π-arene interactions from the flanking rings of *m*-terphenyl isocyanides are commonly encountered when coordinatively unsaturated, low-valent metal centers are generated within these systems.[46,51−56] While such interactions are not observed prior to the formation of **2**, it is important to note that re-exposure of this THF-adduct to an N_2 atmosphere regenerates the terminal dinitrogen complex **1** (Scheme 3). Accordingly, this substitution indicates that the THF ligand is not electronically well matched for the low-valent Fe center, despite being able to stabilize the complex to ligand redistribution processes.

Whereas the four-coordinate complex $Fe(CO)_2(CNAr^{Tripp2})_2$ is not amenable to isolation under the conditions probed, we reasoned that the lability of the N_2 ligand in complex **1** would enable reactivity analogous to $Fe(CO)_4$ in the presence of certain substrates. Accordingly, we engaged complex **1** in a solution-phase reactivity survey with substrates that have been established to react with $Fe(CO)_4$ under matrix conditions, or in experiments where $Fe(CO)_4$ has been proposed to be generated photolytically. For example, exposure of a C_6D_6 solution of **1** to an atmosphere of H_2 led to an immediate lightening in color to pale yellow. ^1H NMR spectroscopic analysis of the reaction mixture revealed the complete conversion to a single new product with a hydride resonance centered at $\delta_H = -9.46$ ppm. In addition, the FTIR spectrum of this mixture showed the disappearance of the ν_{NN} stretch for complex **1**, along with a ca. 25 cm^{-1} blueshift of the asymmetric ν_{CN} stretch. The product was determined by single-crystal X-ray diffraction to be *cis*,*cis*,*trans*-$H_2Fe(CO)_2(CNAr^{Tripp2})_2$ (**3**; Figure 3, Scheme 4), which serves as an important analogue of $H_2Fe(CO)_4$, the first transition-metal hydride complex described in the literature.[57] The dihydride complex $H_2Fe(CO)_4$ was first prepared through the so-called Hieber base reaction between hydroxide (OH^-) and $Fe(CO)_5$,[58] which has been employed for molecular water−gas shift chemistry.[59] Additionally, matrix-isolated $Fe(CO)_4$ was shown to react with H_2 in the first instance of dihydrogen oxidative addition to a metal center under cryogenic conditions.[60] Later, polyethylene film matrix isolation allowed for the thermal reaction between $Fe(N_2)(CO)_4$ and H_2 at 210 K in a more direct analogy to the reaction between **1** and H_2 forming **3**.[50] Importantly, the more sterically protected dihydride **3** retains its integrity at room temperature in both solution and the solid state when exposed to a vacuum. This

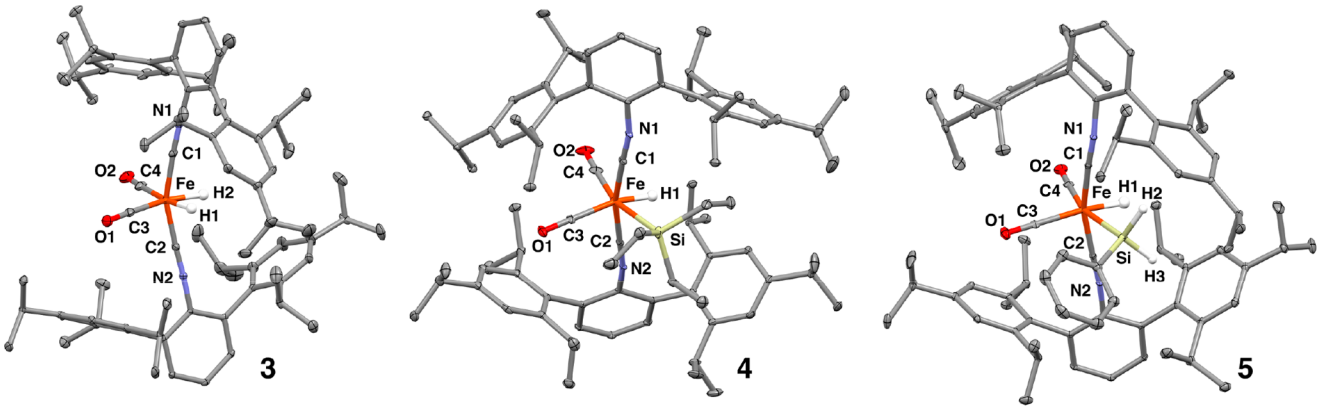

Figure 3. Molecular structure of $H_2Fe(CO)_2(CNAr^{Tripp2})_2$ (**3**, left), $HFe(SiEt_3)(CO)_2(CNAr^{Tripp2})_2$ (**4**, middle), and $HFe(SiH_2Ph)(CO)_2(CNAr^{Tripp2})_2$ (**5**, right).

https://dx.doi.org/10.1021/acs.organomet.0c00487
Organometallics 2020, 39, 3394−3402

Scheme 4. Oxidative Addition Reactions Mediated by Complex 1

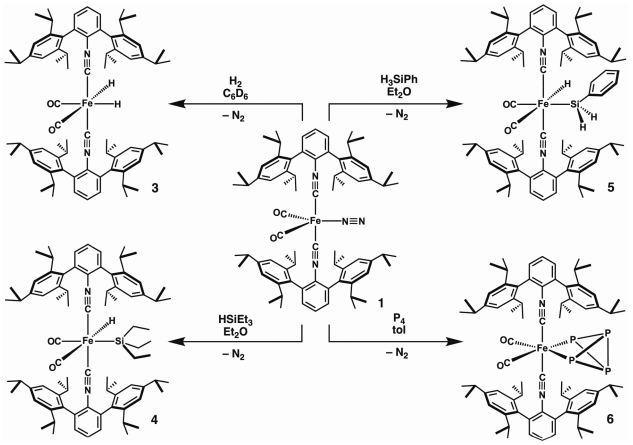

behavior contrasts significantly with that of $H_2Fe(CO)_4$, which liberates dihydrogen above −10 °C. Iron dihydrides of the type $H_2Fe(PR_3)_4$ and $H_2Fe(CO)_2(PR_3)_2$ have been crystallographically characterized; however, an important distinction is that they are derived from hydride and proton sources and not H_2.[61−66]

Unlike with H_2, the direct oxidative addition of silane Si−H bonds by $Fe(CO)_4$ under matrix conditions or in the gas phase has not been reported. However, it has been long established that $Fe(CO)_5$ can mediate olefin hydrosilylation in solution under photolytic conditions in a process proposed to proceed via the intermediacy of the tetracarbonyl $Fe(CO)_4$.[10,11] To provide mechanistic insight into the hydrosilylation process, it has been shown that photolysis of $Fe(CO)_5$ in the presence of $HSiPh_3$, $HSiCl_3$, or $HSiEt_3$ generates the corresponding $HFe(SiR_3)(CO)_4$ complexes, which have been spectroscopically characterized.[26,67,68] In order to obtain more definitive structural information on silyl-hydride compounds of this type, **1** was treated with $HSiEt_3$ at room temperature. Analysis of the reaction mixture by ^{1}H NMR spectroscopy revealed a hydride resonance at δ_H = −9.45 ppm, which is effectively identical to the hydride chemical shift found for the dihydride complex **3**. However, X-ray structural analysis of single crystals grown from a *n*-pentane/Et_2O mixture revealed the product to be the hydrido-silyl complex $HFe(SiEt_3)(CO)_2(CNAr^{Tripp2})_2$ (**4**), which possess a *cis*-disposition of the hydride and silyl ligands (Figure 3, Scheme 4). Relative to **1**, the asymmetric ν_{CN} stretch of **3** shifts 20 cm^{-1} to lower frequency, whereas both ν_{CO} stretches shift by ca. 40 cm^{-1} to higher frequency. Similar results were obtained when the primary silane H_3SiPh was added to **1**, resulting in the clean formation of $HFe(SiH_2Ph)(CO)_2(CNAr^{Tripp2})_2$ (**5**) as confirmed by ^{1}H NMR spectroscopy and X-ray diffraction (Figure 3, Scheme 4). It is worth noting that $Fe(N_2)(CNAr^{Mes2})_4$ has not been observed to oxidatively add H_2 or silanes. This lack of reactivity is presumably a result of the steric congestion imposed by four encumbering *m*-terphenyl isocyanides, which may either block the approach of substrates larger than N_2 or CO to the Fe center or inhibit the structural rearrangements required to accommodate two additional ligands within the primary coordination sphere.

The results above show that complex **1** can replicate the reactivity patterns of $Fe(CO)_4$ with H_2 and silanes following the loss of dinitrogen. Whereas it has been previously demonstrated that these substrates react with $Fe(CO)_4$ in a well-defined manner, we became interested in probing the behavior of **1** toward substrates that have a more ill-defined reactivity profile with $Fe(CO)_4$. As the solution phase reactivity of $Fe(CO)_4$ is commonly accessed via UV-photolysis of $Fe(CO)_5$, it is important to note that its reactivity with photosensitive substrates is either relatively unexplored or proceeds via complex mechanisms involving reactive photoproducts. As an example, it has been long known that photolysis of $Fe(CO)_5$ in the presence of white phosphorus (P_4), which undergoes photolytic cleavage at wavelengths below 300 nm,[69,70] results in complex mixtures of multinuclear and polymeric iron−phosphorus species.[71,72] However, when dinitrogen complex **1** is treated with 1.0 equiv of P_4 in toluene solution, clean conversion to a single new product is observed by ^{1}H NMR and IR spectroscopy. Structural determination by X-ray diffraction on orange crystals of this product revealed it to be the edge-opened P_4 complex, $Fe(\kappa^2\text{-}P_4)(CO)_2(CNAr^{Tripp2})_2$ (**6**; Scheme 4, Figure 4), in which the

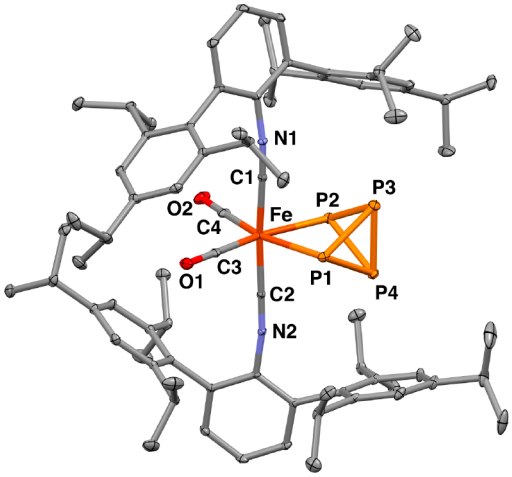

Figure 4. Molecular structure of $Fe(\kappa^2\text{-}P_4)(CO)_2(CNAr^{Tripp2})_2$ (**6**).

FeL_4 fragment is inserted into one P−P bond of the P_4 tetrahedron. This activation mode of white phosphorus has been observed only for Group 4 and Group 9 transition metals[53,73−77] making compound **6** structurally unique among iron-polyphosphorus complexes. However, it is worth noting that three edge-opened P_4 complexes of the formulation $Cp^*Co(\kappa^2\text{-}P_4)L$ (L = CO, NHC, CNR) have been fully characterized,[53,74,76] which is in line with the qualitative isolobal relationship between the $[Fe(CO)_4]$ and $[CpCo(CO)]$ fragments.[78]

CONCLUSIONS

The work presented here shows that the dinitrogen complex $Fe(N_2)(CO)_2(CNAr^{Tripp2})_2$ (**1**) effectively serves as a masked source of a four-coordinate zerovalent iron species analogous to $Fe(CO)_4$. The combined ligand set of CO and $CNAr^{Tripp2}$ effectively deactivates the intramolecular decomposition pathway observed for tetra-isocyanide complex $Fe(N_2)(CNAr^{Mes2})_4$. Additionally, complex **1** is isolobal to matrix-isolated $Fe(N_2)(CO)_4$, and the N_2 ligand of both species has been found to be substitutionally labile. In the absence of an N_2 atmosphere, the dinitrogen ligand in **1** can be substituted by THF, which is an electronically mismatched donor ligand for an electron-rich, zerovalent Fe center and highlights the

https://dx.doi.org/10.1021/acs.organomet.0c00487
Organometallics 2020, 39, 3394−3402

inherent instability of the FeL_4 core in a strongly π-acidic ligand field. In addition, the N_2 ligand within complex **1** can be displaced by substrate molecules. This has been demonstrated by the oxidative addition of E−H bonds (E = H, Si) to the Fe center in **1** and finds analogy to the established chemistry of $Fe(CO)_4$. However, this reactivity contrasts with that of the tetraisocyanide complex, $Fe(N_2)(CNAr^{Mes2})_4$. Evidently, the small steric profile of CO allows complex **1** to undergo the necessary molecular rearrangements for small molecule binding and activation, whereas the more congested $Fe(N_2)(CNAr^{Mes2})_4$ cannot accommodate additional substrates. Accordingly, we describe diamagnetic compound **1** as a masked analogue of $Fe(CO)_4$ in the singlet spin state. Efforts to extend the bond activation processes available to **1** to catalytic systems analogous to the photochemistry of $Fe(CO)_5$ are underway.

EXPERIMENTAL SECTION

General Considerations. All manipulations were carried out under an atmosphere of purified dinitrogen using standard Schlenk and glovebox techniques. Unless otherwise stated, reagent-grade starting materials were purchased from commercial sources and either used as received or purified by standard procedures.[79] Solvents were dried and deoxygenated according to standard procedures.[80] Benzene-d_6 (Cambridge Isotope Laboratories) was distilled from NaK alloy/benzophenone and stored over activated 3 Å molecular sieves for 2 d prior to use. Celite 405 (Fisher Scientific) was dried under a vacuum (24 h) at a temperature above 250 °C and stored in a glovebox prior to use. Compounds $CNAr^{Tripp2}$ and $Fe(N_2)(CO)_2(CNAr^{Tripp2})_2$ were prepared as previously reported.[41,47]

Solution ^1H and $^{13}C\{^1H\}$ NMR spectra were recorded on a Varian 500 MHz spectrometer equipped with a 5 mm X-Sens cold probe and ^{19}F and $^{31}P\{^1H\}$ NMR Spectra were recorded on a JEOL ECA 500 spectrometer equipped with a broadband, inverse-detect 5 mm probe. ^1H and $^{13}C\{^1H\}$ chemical shifts are reported in ppm relative to $SiMe_4$ (^1H and ^{13}C δ = 0.0 ppm) with reference to residual solvent resonances of 7.16 ppm (^1H) and 128.06 ppm (^{13}C) for C_6D_6. ^{19}F NMR chemical shifts were referenced externally to C_6H_5F (δ = −113.11 ppm in C_6D_6).[71] $^{31}P\{^1H\}$ NMR chemical shifts were referenced externally to 85% H_3PO_4 (δ = 0 ppm). FTIR spectra were recorded on a Thermo-Nicolet iS10 FTIR spectrometer. Samples were prepared as C_6D_6 solutions injected into a ThermoFisher solution cell equipped with KBr windows. Solvent peaks were digitally subtracted from all solution FTIR spectra by comparison with an authentic solvent spectrum obtained prior to that of the sample. The following abbreviations were used for the intensities and characteristics of important IR absorption bands: vs = very strong, s = strong, m = medium, w = weak, vw = very weak, sh = shoulder. Combustion analyses were performed by Midwest Micro Laboratories of Indianapolis, IA. For all attempts, material that had been recrystallized from the reaction mixture twice was analyzed for CHN content. Despite multiple attempts to obtain satisfactory analyses, the combustion results were consistently low. We postulate that KI impurity from the synthesis of $Fe(N_2)(CO)(CNAr^{Tripp2})_2$ is carried forward in subsequent reactions. The best combustion analysis results are reported, and full ^1H and $^{13}C\{^1H\}$ NMR spectra are listed in the Supporting Information to establish spectroscopic purity.

Synthesis of $Fe(THF)(CO)_2(CNAr^{Tripp2})_2$ (2) from $Fe(N_2)(CO)_2(CNAr^{Tripp2})_2$ (1). $Fe(N_2)(CO)_2(CNAr^{Tripp2})_2$ (**1**, 0.050 g, 0.043 mmol) was brought into an argon-filled glovebox as a solid. To this solid was added a 1:4 mixture of THF and *n*-pentane. The solution immediately turned dark in color, and was then covered and stored at −35 °C overnight. This process resulted in the deposition of blackish-yellow crystals, which were isolated, subjected to a vacuum briefly, and collected. Yield: 0.035 g; 0.029 mmol; 67%. ^1H NMR (499.8 MHz, THF-d_8, 20 °C) δ = 7.24 (t, J = 7.6 Hz, 2H, *p*-Ph), 7.09 (d, J = 7.6 Hz, 4H, *m*-Ph), 6.98 (s, 8H, *m*-Tripp), 3.63 (br, 4H, THF), 2.88−2.64 (m, 12H, $CH(CH_3)_2$), 1.79 (br, 4H, THF), 1.26 (d, J = 6.9 Hz, 24H, $CH(CH_3)_2$), 1.12 (d, J = 6.9 Hz, 24H, $CH(CH_3)_2$), 1.07 (d, J = 6.8 Hz, 24H, $CH(CH_3)_2$) ppm. $^{13}C\{^1H\}$ NMR (125.7 MHz, THF-d_8, 20 °C) δ = 220.8 (*C*O), 192.5 (*C*NR), 151.4, 149.7, 139.4, 137.6, 133.8, 128.4, 124.2, 70.2, 34.3, 25.3, 24.5, 24.3, 24.2 ppm. FTIR (KBr windows, *n*-pentane, 25 °C) υ_{CN} = 2126 (m), 2079 (vs) cm^{-1}, υ_{CO} = 1957 (s), 1924 (s) cm^{-1}, also 3057 (w), 2960 (vs), 2951 (s), 2870 (s), 2015 (m), 1609 (w), 1573 (w), 1417 (w), 1363 (vw), 1320 (w), 1243 (vw), 1169 (w), 1105 (vw), 1070 (vw), 1051 (vw), 942 (w), 876 (m), 802 (w), 756 (m), 643 (m), 600(s), 598 (sh), 476 (w) cm^{-1}. Anal. Calcd for $C_{80}H_{106}N_2O_3Fe$: C, 80.10; H, 8.91; N, 2.34. Found: C, 76.70; H, 8.59; N, 3.23. For complex **2**, substoichiometric loss of THF likely also contributes to poor combustion analysis results.

Synthesis of $Fe(THF)(CO)_2(CNAr^{Tripp2})_2$ (2) from $K_2[Fe(CO)_2(CNAr^{Tripp2})_2]$. A THF solution of I_2 (0.022 g, 0.089 mmol, 1 mL) was added to a THF solution of $K_2Fe(CO)_2(CNAr^{Tripp2})_2$ (**1**, 0.120 g, 0.099 mmol, 3 mL) upon thawing under an Ar atmosphere. The reaction was stirred at −35 °C for 1 h, during which time the solution turned dark orange. The solvent was removed, and the product was extracted with *n*-pentane. X-ray quality blackish-yellow single crystals were grown from a concentrated solution at −35 °C overnight. Yield: 0.085 g, 0.070 mmol, 80%.

Synthesis of $H_2Fe(CO)_2(CNAr^{Tripp2})_2$ (3). In a J. Young NMR tube, a C_6D_6 solution of $Fe(N_2)(CO)_2(CNAr^{Tripp2})_2$ (**1**, 0.035 g, 0.030 mmol, 0.8 mL) was subjected to two freeze−pump−thaw cycles and was exposed to an atmosphere of H_2. The color quickly lightened to pale yellow. The product mixture was brought back into a nitrogen-filled glovebox, and volatiles were removed in vacuo. Single crystals were grown from *n*-hexane/benzene (20:1, 1.5 mL) at −35 °C overnight. Yield: 0.026 g, 0.023 mmol, 76%. ^1H NMR (499.8 MHz, C_6D_6, 20 °C) δ = 7.23 (s, 8H, *m*-Tripp), 6.98 (d, J = 7.5 Hz, 4H, *m*-Ph), 6.88 (dd, J = 7.9, 7.2 Hz, 2H, *p*-Ph), 2.96 (sept, J = 6.9 Hz, 4H, $CH(CH_3)_2$), 2.71 (sept, J = 6.8 Hz, 8H, $CH(CH_3)_2$), 1.38 (d, J = 6.9 Hz, 24H, $CH(CH_3)_2$), 1.33 (d, J = 6.9 Hz, 24H, $CH(CH_3)_2$), 1.18 (d, J = 6.8 Hz, 24H, $CH(CH_3)_2$), −9.45 (s, 2H, Fe*H*) ppm. $^{13}C\{^1H\}$ NMR (125.7 MHz, C_6D_6, 20 °C) δ = 210.0 (*C*O), 175.5 (*C*NR), 149.3, 146.6, 139.0, 132.7, 129.9, 129.6, 127.2, 121.2, 35.0, 31.4, 24.8, 24.5, 24.2 ppm. FTIR (KBr windows, C_6D_6, 25 °C) υ_{CN} = 2164 (vw), 2102 (vs) cm^{-1}, υ_{CO} = 2009 (s), 1978 (s) cm^{-1}, also 3047 (w), 2962 (vs), 2932 (w), 2870 (s), 1608 (m), 1566 (w), 1543 (w), 1419 (w), 1385 (m), 1363 (w), 1315 (w), 1240 (vw), 1219 (w), 1196 (vw), 1149 (w), 1103 (vw), 1049 (w), 1022 (w), 1006 (w), 960 (vw), 941 (w), 922 (w), 879 (vw), 842 (w), 760 (w), 706 (vw), 671 (w) cm^{-1}. Anal. Calcd for $C_{76}H_{100}N_2O_2Fe$: C, 80.82; H, 8.92; N, 2.48. Found: C, 74.68; 8.48, H; 2.60.

Synthesis of $HFe(SiEt_3)(CO)_2(CNAr^{Tripp2})_2$ (4). To a Et_2O solution of $Fe(N_2)(CO)_2(CNAr^{Tripp2})_2$ (**1**, 0.055 g, 0.048 mmol, 5 mL) was added a Et_2O solution of triethylsilane (0.011 g, 0.096 mmol, 1 mL). The mixture was stirred for 15 min, after which time the solvent and excess silane were removed by vacuum evaporation. The yellow solid was dissolved in *n*-hexane/Et_2O (10:1) for recrystallization at −35 °C overnight producing pale yellow diffraction quality samples. Yield: 0.056 g, 0.045 mmol, 94%. ^1H NMR (499.8 MHz, C_6D_6, 20 °C) δ = 7.26 (s, 8H, *m*-Tripp), 7.01 (d, J = 7.6 Hz, 4H, *m*-Ph), 6.85 (t, J = 7.6 Hz, 2H, *p*-Ph), 2.97 (sept, J = 6.9 Hz, 4H, $CH(CH_3)_2$), 2.78 (sept, J = 6.8 Hz, 8H, $CH(CH_3)_2$), 1.45 (d, J = 6.8 Hz, 24H, $CH(CH_3)_2$), 1.40 (d, J = 6.9 Hz, 24H, $CH(CH_3)_2$), 1.12 (d, J = 6.7 Hz, 24H, $CH(CH_3)_2$), 0.82 (t, J = 7.7 Hz, 9H, $Si(CH_2)_3(CH_3)_3$)), 0.31 (q, J = 7.7 Hz, 6H, $Si(CH_2)_3(CH_3)_3$), −9.45 (s, 1H, Fe*H*) ppm. $^{13}C\{^1H\}$ NMR (125.7 MHz, C_6D_6, 20 °C) δ = 211.2 (*C*O), 178.94, 178.88 (*C*NR), 149.2, 146.5, 138.4, 133.4, 131.2, 130.0, 126.4, 121.6, 34.9, 31.3, 25.6, 24.4, 23.6, 11.0, 9.5 ppm. FTIR (KBr windows, C_6D_6, 25 °C) υ_{CN} = 2118 (w), 2060 (vs) cm^{-1}, υ_{CO} = 1998 (s), 1967 (s) cm^{-1}, also 3051 (w), 2956 (vs), 2934 (s), 2905 (s), 2870 (s), 1608 (m), 1566 (w), 1543 (w), 1415 (w), 1385 (w), 1362 (w), 1319 (w), 1238 (vw), 1196 (vw), 1149 (w), 1103 (vw), 1053 (vw), 1006 (w), 941 (w), 921 (w), 875 (w), 760 (w), 679 (w), 571 (m) cm^{-1}. Anal. Calcd for $C_{82}H_{114}N_2O_2SiFe$: C, 79.19; H, 9.24; N, 2.25. Found: C, 76.24; 9.34, H, 2.67.

https://dx.doi.org/10.1021/acs.organomet.0c00487
Organometallics 2020, 39, 3394−3402

Synthesis of $HFe(SiH_2Ph)(CO)_2(CNAr^{Tripp2})_2$ (5). To a Et_2O solution of $Fe(N_2)(CO)_2(CNAr^{Tripp2})_2$ (**1**, 0.105 g, 0.091 mmol, 6 mL) was added a Et_2O solution of H_3SiPh (0.020 g, 0.182 mmol, 2 mL). The mixture was stirred for 15 min, after which time the solvent and excess silane were removed by a vacuum. Dissolution of the product in *n*-hexane/benzene and storage at −35 °C for 3 d deposited yellow crystals. Yield: 0.099 g, 0.079 mmol, 87%. ^{1}H NMR (499.8 MHz, C_6D_6, 20 °C) δ = 7.33 (d, J = 6.4 Hz, 2H, *o*-PhSi), 7.23 (s, 8H, *m*-Tripp), 6.98 (d, J = 7.6 Hz, 4H, *m*-Ph), 6.86 (t, J = 7.6 Hz, 2H, *p*-Ph), 3.63 (dd, J = 2.3 Hz, 2H, SiH_2), 2.96 (sept, J = 6.9 Hz, 4H, $CH(CH_3)_2$), 2.73 (sept, J = 6.8 Hz, 8H, $CH(CH_3)_2$), 1.39 (d, J = 6.9 Hz, 24H, $CH(CH_3)_2$), 1.30 (d, J = 6.9 Hz, 24H, $CH(CH_3)_2$), 1.13 (d, J = 6.8 Hz, 24H, $CH(CH_3)_2$), −9.96 (t, J = 1.9 Hz, 1H, Fe*H*) ppm. The *m*- and *p*-PhSi protons were obscured by *m*-terphenyl resonances. $^{13}C\{^1H\}$ NMR (125.7 MHz, C_6D_6, 20 °C) δ = 209.5 (CO), 175.5 (*C*NR), 149.3, 146.4, 142.3, 139.0, 135.8, 132.9, 130.3, 129.8, 127.4, 127.2, 127.0, 121.6, 35.1, 31.3, 25.0, 24.5, 23.9 ppm. FTIR (KBr windows, C_6D_6, 25 °C) υ_{CN} = 2135 (sh), 2090 (vs) cm^{-1}, υ_{CO} = 2013 (s), 1981 (s) cm^{-1}, also 3047 (w), 2960 (vs), 2930 (s), 2904 (m), 2869 (s), 1608 (m), 1570 (w), 1542 (w), 1461 (m), 1427 (w), 1415 (w), 1385 (w), 1362 (w), 1319 (w), 1241 (vw), 1103 (vw), 1052 (w), 941 (m), 922 (w), 876 (w), 833 (w), 760 (w), 725 (vw), 698 (vw), 679 (vw), 640 (vw), 598 (m) cm^{-1}. Anal. Calcd for $C_{82}H_{106}N_2O_2SiFe$: C, 79.70; H, 8.65; N, 2.27. Found: C, 76.94; 8.84, H, 2.00.

Synthesis of $Fe(\kappa^2\text{-}P_4)(CO)_2(CNAr^{Tripp2})_2$ (6). To a thawing toluene solution of $Fe(N_2)(CO)_2(CNAr^{Tripp2})_2$ (**1**, 0.095 g, 0.082 mmol, 4 mL) was added a toluene solution of P_4 (0.015 g, 0.123 mmol, 4 mL). The reaction mixture was stirred for 40 min, during which time the solution turned from orange-yellow to red-orange. The solvent was evaporated to dryness, and the resulting solid was recrystallized from *n*-pentane (2 mL) at −35 °C over 12 h to give orange single. Yield: 0.089 g, 0.070 mmol, 86% ^{1}H NMR (499.8 MHz, C_6D_6, 20 °C) δ = 7.28 (s, 8H, *m*-Tripp), 7.07 (d, J = 7.6 Hz, 4H, *m*-Ph), 6.92 (t, J = 7.6 Hz, 2H, *p*-Ph), 2.97−2.85 (m, 12H, $CH(CH_3)_2$), 1.52 (d, J = 6.9 Hz, 24H, $CH(CH_3)_2$), 1.31 (d, J = 6.9 Hz, 24H, $CH(CH_3)_2$), 1.17 (d, J = 6.8 Hz, 24H, $CH(CH_3)_2$) ppm. $^{13}C\{^1H\}$ NMR (125.7 MHz, C_6D_6, 20 °C) δ = 208.2 (CO), 170.2 (*C*NR), 149.6, 146.5, 139.6, 133.1, 130.7, 129.6, 127.6, 122.2, 35.1, 31.6, 25.0, 24.37, 24.34 ppm. $^{31}P\{^1H\}$ NMR (202.7 MHz, C_6D_6, 20 °C) δ = −254.0 (br s, 2P), −335.3 (br s, 2P) ppm. FTIR (KBr windows, C_6D_6, 25 °C) υ_{CN} = 2129 (m), 2090 (vs) cm^{-1}, υ_{CO} = 2009 (s), 1968 (s) cm^{-1}, also 3047 (w), 2960 (vs), 2931 (s), 2904 (m), 2870 (s), 1608 (m), 1569 (w), 1542 (w), 1466 (w), 1415 (vw), 1384 (w), 1361 (vw), 1315 (w), 1261 (vw), 1238 (vw), 1196 (vw), 1149 (vw), 1103 (vw), 1053 (vw), 1018 (w), 941 (w), 922 (w), 879 (w), 760 (w), 732 (vw), 571 (w) cm^{-1}. Despite attempts, satisfactory combustion analysis was not obtained.

Crystallographic Structure Determinations. Single X-ray structure determinations were performed at 100 K on Bruker Kappa diffractometers equipped with Mo radiation source and an APEX-II CCD area detector. All structures were solved via direct methods with SHELXS[81] and refined by full-matrix least-squares procedures using SHELXL[81] within the Olex2[82] software. Full details for data collection and refinement can be found in the Supporting Information.

■ ASSOCIATED CONTENT

Supporting Information

The Supporting Information is available free of charge at https://pubs.acs.org/doi/10.1021/acs.organomet.0c00487.

Representative ^{1}H, $^{13}C\{^1H\}$, and $^{31}P\{^1H\}$ NMR spectra, and results of single-crystal diffraction experiments (PDF)

Accession Codes

CCDC 2016082−2016086 contain the supplementary crystallographic data for this paper. These data can be obtained free of charge via www.ccdc.cam.ac.uk/data_request/cif, or by emailing data_request@ccdc.cam.ac.uk, or by contacting The Cambridge Crystallographic Data Centre, 12 Union Road, Cambridge CB2 1EZ, UK; fax: +44 1223 336033.

■ AUTHOR INFORMATION

Corresponding Author

Joshua S. Figueroa − *Department of Chemistry and Biochemistry, University of California, San Diego, La Jolla, California 92093, United States;* orcid.org/0000-0003-2099-5984; Email: jsfig@ucsd.edu

Authors

Myles J. Drance − *Department of Chemistry and Biochemistry, University of California, San Diego, La Jolla, California 92093, United States;* orcid.org/0000-0003-1682-9828

Shuai Wang − *Department of Chemistry and Biochemistry, University of California, San Diego, La Jolla, California 92093, United States;* orcid.org/0000-0001-9464-6758

Milan Gembicky − *Department of Chemistry and Biochemistry, University of California, San Diego, La Jolla, California 92093, United States;* orcid.org/0000-0002-3898-1612

Arnold L. Rheingold − *Department of Chemistry and Biochemistry, University of California, San Diego, La Jolla, California 92093, United States;* orcid.org/0000-0003-4472-8127

Complete contact information is available at: https://pubs.acs.org/10.1021/acs.organomet.0c00487

Notes

The authors declare no competing financial interest.

■ ACKNOWLEDGMENTS

We are grateful to the U.S. National Science Foundation (CHE-1802646) for support of this work. M.J.D. thanks the UCSD Department of Chemistry and Biochemistry for a Distinguished Graduate Student Fellowship (2018−2019).

■ REFERENCES

(1) Wrighton, M. Photochemistry of Metal Carbonyls. *Chem. Rev.* **1974**, *74*, 401−430.

(2) Poliakoff, M. II. $Fe(CO)_4$. *Chem. Soc. Rev.* **1978**, *7*, 527−540.

(3) Poliakoff, M.; Weitz, E. Shedding Light on Organometallic Reactions: the Characterization of Tetracarbonyliron ($Fe(CO)_4$), a Prototypical Reaction Intermediate. *Acc. Chem. Res.* **1987**, *20*, 408−414.

(4) Mond, L.; Quincke, F. LV.—Note on a Volatile Compound of Iron with Carbonic Oxide. *J. Chem. Soc., Trans.* **1891**, *59* (0), 604−607.

(5) Mond, L.; Langer, C. On Iron Carbonyls. *J. Chem. Soc., Trans.* **1891**, *59*, 1090−1093.

(6) Dewar, J.; Jones, H. O. The Physical and Chemical Properties of Iron Carbonyl. *Proc. R. Soc. London A* **1905**, *76*, 558−577.

(7) Booth, B. L.; Goldwhite, H.; Haszeldine, R. N. Metal Carbonyl Chemistry. Part III. Iron Pentacarbonyl as a Hydroformylation Catalyst. *J. Chem. Soc. C* **1966**, 1447−1449.

(8) Harmon, R. E.; Gupta, S. K.; Brown, D. J. Hydrogenation of Organic Compounds Using Homogeneous Catalysts. *Chem. Rev.* **1973**, *73*, 21−52.

(9) Schroeder, M. A.; Wrighton, M. S. Pentacarbonyliron(0) Photocatalyzed Hydrogenation and Isomerization of Olefins. *J. Am. Chem. Soc.* **1976**, *98*, 551−558.

(10) Schroeder, M. A.; Wrighton, M. S. Pentacarbonyliron(0) Photocatalyzed Reactions of Trialkylsilanes with Alkenes. *J. Organomet. Chem.* **1977**, *128*, 345−358.

(11) Mitchener, J. C.; Wrighton, M. S. Photogeneration of Very Active Homogeneous Catalysts Using Laser Light Excitation of Iron Carbonyl Precursors. *J. Am. Chem. Soc.* **1981**, *103*, 975−977.
(12) Poliakoff, M.; Turner, J. J. Infrared Spectra and Photochemistry of the Complex Pentacarbonyliron in Solid Matrices at 4 and 20 K: Evidence for Formation of the Complex Tetracarbonyliron. *J. Chem. Soc., Dalton Trans.* **1973**, 1351−1357.
(13) Poliakoff, M.; Turner, J. J. Structure and Reactions of Matrix-Isolated Tetracarbonyliron(0). *J. Chem. Soc., Dalton Trans.* **1974**, 2276−2285.
(14) Davies, B.; McNeish, A.; Poliakoff, M.; Turner, J. J. The Infrared Laser Induced Isomerization of Iron Tetracarbonyl. the First Non-Berry Pseudorotation. *J. Am. Chem. Soc.* **1977**, *99*, 7573−7579.
(15) Weitz, E. Transient Infrared Spectroscopy as a Probe of Coordinatively Unsaturated Metal Carbonyls in the Gas Phase. *J. Phys. Chem.* **1994**, *98*, 11256−11264.
(16) Ihee, H.; Cao, J.; Zewail, A. H. Ultrafast Electron Diffraction: Structures in Dissociation Dynamics of $Fe(CO)_5$. *Chem. Phys. Lett.* **1997**, *281*, 10−19.
(17) Ihee, H.; Cao, J.; Zewail, A. H. Ultrafast Electron Diffraction of Transient $[Fe(CO)_4]$: Determination of Molecular Structure and Reaction Pathway. *Angew. Chem., Int. Ed.* **2001**, *40*, 1532−1536.
(18) Poliakoff, M.; Turner, J. J. The Structure of $[Fe(CO)_4]$—an Important New Chapter in a Long-Running Story. *Angew. Chem., Int. Ed.* **2001**, *40*, 2809−2812.
(19) Besora, M.; Carreon-Macedo, J.-L.; Cimas, Á.; Harvey, J. N. Spin-State Changes and Reactivity in Transition Metal Chemistry: Reactivity of Iron Tetracarbonyl. *Adv. Inorg. Chem.* **2009**, *61*, 573−623.
(20) Lomont, J. P.; Nguyen, S. C.; Harris, C. B. Ultrafast Infrared Studies of the Role of Spin States in Organometallic Reaction Dynamics. *Acc. Chem. Res.* **2014**, *47*, 1634−1642.
(21) Burdett, J. K. Calculation of the Geometries of Binary Transition Metal Carbonyl and Dinitrogen Complexes. *J. Chem. Soc., Faraday Trans. 2* **1974**, *70*, 1599−1613.
(22) Burdett, J. K. New Method for the Determination of the Geometries of Binary Transition Metal Complexes. *Inorg. Chem.* **1975**, *14*, 375−382.
(23) Elian, M.; Hoffmann, R. Bonding Capabilities of Transition Metal Carbonyl Fragments. *Inorg. Chem.* **1975**, *14*, 1058−1076.
(24) House, P. G.; Weitz, E. Reactions of Molecular Nitrogen and Triethylamine with Coordinatively Unsaturated Iron Carbonyls: Spin Effects on Reactions. *Chem. Phys. Lett.* **1997**, *266*, 239−245.
(25) Leadbeater, N. Enlightening Organometallic Chemistry: the Photochemistry of $Fe(CO)_5$ and the Reaction Chemistry of Unsaturated Iron Carbonyl Fragments. *Coord. Chem. Rev.* **1999**, *188*, 35−70.
(26) Snee, P. T.; Payne, C. K.; Kotz, K. T.; Yang, H.; Harris, C. B. Triplet Organometallic Reactivity Under Ambient Conditions: an Ultrafast UV Pump/IR Probe Study. *J. Am. Chem. Soc.* **2001**, *123*, 2255−2264.
(27) Portius, P.; Yang, J.; Sun, X.-Z.; Grills, D. C.; Matousek, P.; Parker, A. W.; Towrie, M.; George, M. W. Unraveling the Photochemistry of $Fe(CO)_5$ in Solution: Observation of $Fe(CO)_3$ and the Conversion Between $^3Fe(CO)_4$ and $^1Fe(CO)_4$(Solvent. *J. Am. Chem. Soc.* **2004**, *126*, 10713−10720.
(28) Besora, M.; Carreon-Macedo, J.-L.; Cowan, A. J.; George, M. W.; Harvey, J. N.; Portius, P.; Ronayne, K. L.; Sun, X.-Z.; Towrie, M. A. Combined Theoretical and Experimental Study on the Role of Spin States in the Chemistry of $Fe(CO)_5$ Photoproducts. *J. Am. Chem. Soc.* **2009**, *131*, 3583−3592.
(29) Hoberg, H.; Jenni, K.; Angermund, K.; Krüger, C. CC-Linkages of Ethene with CO_2 on an Iron(0) Complex—Synthesis and Crystal Structure Analysis of $[(PEt_3)_2Fe(C_2H_4)_2]$. *Angew. Chem., Int. Ed. Engl.* **1987**, *26*, 153−155.
(30) Geier, S.; Goddard, R.; Holle, S.; Jolly, P. W.; Krüger, C.; Lutz, F. Reaction of Unconjugated Dienes with $[Fe(R_2P(CH_2)_nPR_2)]$ Species. *Organometallics* **1997**, *16*, 1612−1620.
(31) Lavallo, V.; El-Batta, A.; Bertrand, G.; Grubbs, R. H. Insights Into the Carbene-Initiated Aggregation of $[Fe(Cot)_2]$. *Angew. Chem., Int. Ed.* **2011**, *50*, 268−271.
(32) Zhang, H.; Ouyang, Z.; Liu, Y.; Zhang, Q.; Wang, L.; Deng, L. (Aminocarbene)(Divinyltetramethyldisiloxane)Iron(0) Compounds: a Class of Low-Coordinate Iron(0) Reagents. *Angew. Chem., Int. Ed.* **2014**, *53*, 8432−8436.
(33) Hickey, A. K.; Lee, W.-T.; Chen, C.-H.; Pink, M.; Smith, J. M. A Bidentate Carbene Ligand Stabilizes a Low-Coordinate Iron(0) Carbonyl Complex. *Organometallics* **2016**, *35*, 3069−3073.
(34) Burcher, B.; Sanders, K. J.; Benda, L.; Pintacuda, G.; Jeanneau, E.; Danopoulos, A. A.; Braunstein, P.; Olivier-Bourbigou, H.; Breuil, P.-A. R. A Straightforward Access to Stable, 16 Valence-Electron Phosphine-Stabilized Fe0 Olefin Complexes and Their Reactivity. *Organometallics* **2017**, *36*, 605−613.
(35) Casitas, A.; Krause, H.; Lutz, S.; Goddard, R.; Bill, E.; Fürstner, A. Ligand Exchange on and Allylic C−H Activation by Iron(0) Fragments: π-Complexes, Allyliron Species, and Metallacycles. *Organometallics* **2018**, *37*, 729−739.
(36) Labios, L. A.; Millard, M. D.; Rheingold, A. L.; Figueroa, J. S. Bond Activation, Substrate Addition and Catalysis by an Isolable Two-Coordinate Pd(0) Bis-Isocyanide Monomer. *J. Am. Chem. Soc.* **2009**, *131*, 11318−11319.
(37) Fox, B. J.; Millard, M. D.; DiPasquale, A. G.; Rheingold, A. L.; Figueroa, J. S. Thallium(I) as a Coordination Site Protection Agent: Preparation of an Isolable Zero-Valent Nickel Tris-Isocyanide. *Angew. Chem., Int. Ed.* **2009**, *48*, 3473−3477.
(38) Margulieux, G. W.; Weidemann, N.; Lacy, D. C.; Moore, C. E.; Rheingold, A. L.; Figueroa, J. S. Isocyano Analogues of $[Co(CO)_4]^n$: a Tetraisocyanide of Cobalt Isolated in Three States of Charge. *J. Am. Chem. Soc.* **2010**, *132*, 5033−5035.
(39) Agnew, D. W.; Moore, C. E.; Rheingold, A. L.; Figueroa, J. S. Kinetic Destabilization of Metal-Metal Single Bonds: Isolation of a Pentacoordinate Manganese(0) Monoradical. *Angew. Chem., Int. Ed.* **2015**, *54*, 12673−12677.
(40) Cotton, F. A.; Zingales, F. The Donor-Acceptor Properties of Isonitriles as Estimated by Infrared Study. *J. Am. Chem. Soc.* **1961**, *83* (2), 351−355.
(41) Carpenter, A. E.; Mokhtarzadeh, C. C.; Ripatti, D. S.; Havrylyuk, I.; Kamezawa, R.; Moore, C. E.; Rheingold, A. L.; Figueroa, J. S. Comparative Measure of the Electronic Influence of Highly Substituted Aryl Isocyanides. *Inorg. Chem.* **2015**, *54*, 2936−2944.
(42) Agnew, D. W.; Moore, C. E.; Rheingold, A. L.; Figueroa, J. S. Comparison of Nucleophilic- and Radical-Based Routes to the Formation of Manganese-Main Group Element Single Bonds. *Dalton Trans.* **2017**, *46*, 6700−6707.
(43) Chan, C.; Carpenter, A. E.; Gembicky, M.; Moore, C. E.; Rheingold, A. L.; Figueroa, J. S. Associative Ligand Exchange and Substrate Activation Reactions by a Zero-Valent Cobalt Tetraisocyanide Complex. *Organometallics* **2019**, *38*, 1436−1444.
(44) Emerich, B. M.; Moore, C. E.; Fox, B. J.; Rheingold, A. L.; Figueroa, J. S. Protecting-Group-Free Access to a Three-Coordinate Nickel(0) Tris-Isocyanide. *Organometallics* **2011**, *30*, 2598−2608.
(45) Whitmire, K. H.; Lee, T. R.; Lewis, E. S. Kinetics and Mechanism of the Reaction of $[Et_4N][HFe(CO)_4]$ and Alkyl Halides. the Unexpected Formation of Acetone. *Organometallics* **1986**, *5*, 987−994.
(46) Mokhtarzadeh, C. C.; Margulieux, G. W.; Carpenter, A. E.; Weidemann, N.; Moore, C. E.; Rheingold, A. L.; Figueroa, J. S. Synthesis and Protonation of an Encumbered Iron Tetraisocyanide Dianion. *Inorg. Chem.* **2015**, *54*, 5579−5587.
(47) Drance, M. J.; Sears, J. D.; Mrse, A. M.; Moore, C. E.; Rheingold, A. L.; Neidig, M. L.; Figueroa, J. S. Terminal Coordination of Diatomic Boron Monofluoride to Iron. *Science* **2019**, *363*, 1203−1205.
(48) *Cambridge Structural Database (CSD)*, version 5.41 (November 2019).

https://dx.doi.org/10.1021/acs.organomet.0c00487
Organometallics 2020, 39, 3394−3402

(49) Hazari, N. Homogeneous Iron Complexes for the Conversion of Dinitrogen Into Ammonia and Hydrazine. *Chem. Soc. Rev.* **2010**, *39*, 4044−4056.
(50) Cooper, A. I.; Poliakoff, M. High-Pressure Reactions in Polyethylene Films, a New Development in Matrix Isolation. the Photochemical Reaction of $Fe(CO)_5$ with N_2 and the Thermal Reaction of $Fe(CO)_4(N_2)$ with H_2. *Chem. Phys. Lett.* **1993**, *212*, 611−616.
(51) Carpenter, A. E.; Margulieux, G. W.; Millard, M. D.; Moore, C. E.; Weidemann, N.; Rheingold, A. L.; Figueroa, J. S. Zwitterionic Stabilization of a Reactive Cobalt Tris-Isocyanide Monoanion by Cation Coordination. *Angew. Chem., Int. Ed.* **2012**, *51*, 9412−9416.
(52) Ditri, T. B.; Carpenter, A. E.; Ripatti, D. S.; Moore, C. E.; Rheingold, A. L.; Figueroa, J. S. Chloro- and Trifluoromethyl-Substituted Flanking-Ring M-Terphenyl Isocyanides: H 6-Arene Binding to Zero-Valent Molybdenum Centers and Comparison to Alkyl-Substituted Derivatives. *Inorg. Chem.* **2013**, *52*, 13216−13229.
(53) Mokhtarzadeh, C. C.; Rheingold, A. L.; Figueroa, J. S. Dinitrogen Binding, P 4-Activation and Aza-Büchner Ring Expansions Mediated by an Isocyano Analogue of the CpCo(CO) Fragment. *Dalton Trans.* **2016**, *45*, 14561−14569.
(54) Carpenter, A. E.; Rheingold, A. L.; Figueroa, J. S. A. Well-Defined Isocyano Analogue of $HCo(CO)_4$. 1: Synthesis, Decomposition, and Catalytic 1,1-Hydrogenation of Isocyanides. *Organometallics* **2016**, *35*, 2309−2318.
(55) Barnett, B. R.; Labios, L. A.; Stauber, J. M.; Moore, C. E.; Rheingold, A. L.; Figueroa, J. S. Synthetic and Mechanistic Interrogation of Pd/Isocyanide-Catalyzed Cross-Coupling: Π-Acidic Ligands Enable Self-Aggregating Monoligated Pd(0) Intermediates. *Organometallics* **2017**, *36*, 944−954.
(56) Mokhtarzadeh, C. C.; Carpenter, A. E.; Spence, D. P.; Melaimi, M.; Agnew, D. W.; Weidemann, N.; Moore, C. E.; Rheingold, A. L.; Figueroa, J. S. Geometric and Electronic Structure Analysis of the Three-Membered Electron-Transfer Series $[(M\text{-}CNR)_2[CpCo]_2]^n$ (n = 0, 1−, 2−) and Its Relevance to the Classical Bridging-Carbonyl System. *Organometallics* **2017**, *36*, 2126−2140.
(57) Heiber, W.; Leutert, F. Äthylendiamin-Substituierte Eisencarboyle Und Eine Neue Bildungsweise Von Eisencarbonylwasserstoff (XI. Mitteil. Über Metallcarbonyle). *Ber. Dtsch. Chem. Ges. B* **1931**, *64*, 2832−2839.
(58) Hieber, W.; Leutert, F. Uber Metallcarbonyle. XII. Die Basenreaktion Des Eisenpentacarbonyls Und Die Bildung Des Eisencarbonylwasserstoffs. *Z. Anorg. Allg. Chem.* **1932**, *204*, 145−164.
(59) Jacobs, G.; Davis, B. H. Low Temperature Water-Gas Shift Catalysts. In *Catalysis*; Royal Society of Chemistry: Cambridge, 2007; Vol. *20*, pp 122−285.
(60) Sweany, R. L. Matrix Photolysis of Tetracarbonyldihydridoiron. Evidence for Oxidative Addition of Dihydrogen on Tetracarbonyliron. *J. Am. Chem. Soc.* **1981**, *103*, 2410−2412.
(61) Guggenberger, L. J.; Titus, D. D.; Flood, M. T.; Marsh, R. E.; Orio, A. A.; Gray, H. B. Structure of Cis-Dihydridotetrakis(Diethyl Phenylphosphonite)Iron(II). *J. Am. Chem. Soc.* **1972**, *94*, 1135−1143.
(62) Brunet, J.-J.; Kindela, F. B.; Labroue, D.; Neibecker, D. High Yield Synthesis of Cis-Dihydrido-Trans-Bis(Phosphite)-Dicarbonyliron Complexes $H_2Fe(CO)_2[P(OR)_3]_2$ (R = Me, Et, Ph). *Inorg. Chem.* **1990**, *29*, 4152−4153.
(63) Arion, V.; Brunet, J.-J.; Neibecker, D. Crystal Structure, Mössbauer Spectra, and Thermal Behavior of $H_2Fe(CO)_2[P(OPh)_3]_2$. *Inorg. Chem.* **2001**, *40*, 2628−2630.
(64) Summerscales, O. T.; Scott, B. L.; Viswanathan, H. S.; Sutton, A. D. Synthesis and Reactivity of Cis -$FeH_2(Dcpe)_2$ (Dcpe = 1,2-Bis(Dicyclohexylphosphino)Ethane). *Inorg. Chem. Commun.* **2016**, *63*, 57−60.
(65) Maser, L.; Flosdorf, K.; Langer, R. Synthesis and Reactivity of Iron(II) Hydride Complexes Containing Diphenylphosphine Ligands. *J. Organomet. Chem.* **2015**, *791*, 6−12.
(66) Brunet, J.-J.; Chauvin, R.; Donnadieu, B.; Leglaye, P.; Neibecker, D. Improved Synthesis of KHCr(CO)5 and Comparative Coordination Chemistry From $KHCr(CO)_5$ and $KHFe(CO)_4$. *J. Organomet. Chem.* **1998**, *571*, 7−13.
(67) Jetz, W.; Graham, W. A. G. Trichlorosilyl Hydrides of Transition Metals. *J. Am. Chem. Soc.* **1969**, *91*, 3375−3376.
(68) Graham, W. A. G.; Jetz, W. Silicon-Transition Metal Chemistry. I. Photochemical Preparation of Silyl(Transition Metal) Hydrides. *Inorg. Chem.* **1971**, *10*, 4−9.
(69) Rathenau, G. Optische Und Photochemische Versuche Mit Phosphor. *Physica* **1937**, *4*, 503−514.
(70) Tofan, D.; Cummins, C. C. Photochemical Incorporation of Diphosphorus Units Into Organic Molecules. *Angew. Chem., Int. Ed.* **2010**, *49*, 7516−7518.
(71) Schmid, G.; Kempny, H. P. Die Verwendung Von Elementarem Phosphor Als Ligand in Eisencarbonylen. *Z. Anorg. Allg. Chem.* **1977**, *432*, 160−166.
(72) Scheer, M.; Dargatz, M.; Schenzel, K.; Jones, P. G. P4-Liganden Mit Maximaler Elektronendonorfähigkeit: II. $[Fe(CO)_4(M\text{-}P_2)_2\mu\text{-}Fe_2(CO)_{62}]$—Ein Komplex Mit Einer Ungewöhnlich Stabilisierten P4-Einheit. *J. Organomet. Chem.* **1992**, *435*, 123−132.
(73) Scherer, O. J.; Swarowsky, M.; Swarowsky, H.; Wolmershäuser, G. P. Isomers as Complex Ligands. *Angew. Chem., Int. Ed. Engl.* **1988**, *27*, 694−695.
(74) Scherer, O. J.; Swarowsky, M.; Wolmershaeuser, G. Synthesis and Structure of the Cobaltatetraphosphatricycloalkanes $[(.Eta.5\text{-}C_5Me_5)(CO)CoP_4]$ and $[(.Eta.5\text{-}C_5Me_5)_2(CO)_2Co_2P_4]$. *Organometallics* **1989**, *8* (3), 841−842.
(75) Yakhvarov, D.; Barbaro, P.; Gonsalvi, L.; Mañas Carpio, S.; Midollini, S.; Orlandini, A.; Peruzzini, M.; Sinyashin, O.; Zanobini, F. A Snapshot of P4 Tetrahedron Opening: Rh- and Ir-Mediated Activation of White Phosphorus. *Angew. Chem., Int. Ed.* **2006**, *45*, 4182−4185.
(76) Dürr, S.; Ertler, D.; Radius, U. Symmetrical P_4 Cleavage at Cobalt: Characterization of Intermediates on the Way From P_4 to Coordinated P_2 Units. *Inorg. Chem.* **2012**, *51*, 3904−3909.
(77) Seitz, A. E.; Vogel, U.; Eberl, M.; Eckhardt, M.; Balázs, G.; Peresypkina, E. V.; Bodensteiner, M.; Zabel, M.; Scheer, M. Coordination Behavior of $[Cp''_2Zr(\eta 1{:}1\text{-}P_4)]$ Towards Different Lewis Acids. *Chem. - Eur. J.* **2017**, *23*, 10319−10327.
(78) Hoffmann, R. Building Bridges Between Inorganic and Organic Chemistry (Nobel Lecture). *Angew. Chem., Int. Ed. Engl.* **1982**, *21*, 711−724.
(79) Armarego, W. L. F.; Chai, C. L. L. *Purification of Laboratory Chemicals*, 5th ed.; Elsevier, 2003.
(80) Pangborn, A. B.; Giardello, M. A.; Grubbs, R. H.; Rosen, R. K.; Timmers, F. J. Safe and Convenient Procedure for Solvent Purification. *Organometallics* **1996**, *15*, 1518−1520.
(81) Sheldrick, G. M. Crystal Structure Refinement with SHELXL. *Acta Crystallogr., Sect. C: Struct. Chem.* **2015**, *C72*, 3−8.
(82) Dolomanov, O. V.; Bourhis, L. J.; Gildea, R. J.; Howard, J. A. K.; Puschmann, H. OLEX2: a Complete Structure Solution, Refinement and Analysis Program. *J. Appl. Crystallogr.* **2009**, *42*, 339−341.

https://dx.doi.org/10.1021/acs.organomet.0c00487
Organometallics 2020, 39, 3394−3402